Inhibition of the Prohormone Convertase Subtilisin-Kexin Isoenzyme-1 Induces Apoptosis in Human Melanoma Cells

Nina Weiß [1], Agatha Stegemann[1], Marwa A.T. Elsayed[2], Karin U. Schallreuter[2,3], Thomas A. Luger[1], Karin Loser[1], Dieter Metze[1], Carsten Weishaupt[1] and Markus Böhm[1]

Prohormone convertases (PCs) are endoproteases that process many substrates in addition to hormone precursors. Although overexpression of PCs is linked to carcinogenesis in some solid tumors, the role of subtilisin-kexin isoenzyme-1 (SKI-1) in this context is unknown. We show that SKI-1 is constitutively expressed in human pigment cells with higher SKI activity in seven out of eight melanoma cell lines compared with normal melanocytes. SKI-1 immunoreactivity is also detectable in tumor cells of melanoma metastases. Moreover, tissue samples of the latter display higher SKI-1 mRNA levels and activity than normal skin. From various stimuli tested, 12-O-tetradecanoylphorbol-13-acetate and tunicamycin affected SKI-1 expression. Importantly, SKI-1 inhibition by the cell-permeable enzyme inhibitor decanoyl-RRLL-chloromethylketone (dec-RRLL-CMK) not only suppressed proliferation and metabolic activity of melanoma cells *in vitro* but also reduced tumor growth of melanoma cells injected intracutaneously into immunodeficient mice. Mechanistic studies revealed that dec-RRLL-CMK induces classical apoptosis of melanoma cells *in vitro* and affects expression of several SKI-1 target genes including activating transcription factor 6 (ATF6). However, *ATF6* gene silencing does not result in apoptosis of melanoma cells, suggesting that dec-RRLL-CMK induces cell death in an ATF6-independent manner. Our findings encourage further studies on SKI-1 as a potential target for melanoma therapy.

Journal of Investigative Dermatology (2014) **134,** 168–175; doi:10.1038/jid.2013.282; published online 25 July 2013

INTRODUCTION

Prohormone convertases (PCs) are evolutionary conserved serine proteases that were initially characterized as enzymes processing precursor hormones such as proopiomelanocortin or proenkephalin (Seidah and Chrétien, 1999a; Seidah, 2011). They include PC1/3, furin, PC4, PC5/6, paired basic amino acid cleaving enzyme 4, PC7, subtilisin-kexin isoenzyme-1 (SKI-1), and PC subtilisin/kexin 9. The first seven of these PCs cleave substrates within the motif (K/R)–$(X)_n$–(K/R)↓, where $n=0$, 2, 4, or 6 and X is any amino acid except Cys. SKI-1 cleaves at the consensus motif (R/K)–*X*–(hydrophobic)–*X*, where *X* is variable (Pasquato *et al.*, 2006), whereas PC subtilisin/kexin 9 cleaves behind VFAQ↓ (Benjannet *et al.*, 2004).

SKI-1 belongs to the most recently discovered PCs (Seidah *et al.*, 1999b). It regulates cartilage development (Schlombs *et al.*, 2003), bone mineralization (Gorski *et al.*, 2009), and processing of viral glycoproteins, e.g., those of Lassa virus (Lenz *et al.*, 2001). SKI-1 activates the sterol regulatory element binding proteins 1 and 2 (Espenshade *et al.*, 1999); hence, it is a key regulator of lipid metabolism. Accordingly, pharmacological inhibitors are being developed for the future treatment of dyslipidemia (Seidah and Prat, 2007). The essential role for SKI-1 is highlighted by genetic ablation studies. Here, global SKI-1 deficiency leads to early embryonic death of mice (Yang *et al.*, 2001).

In this study, we investigated the expression, regulation, and function of SKI-1 in normal human melanocytes (NHMs) and melanoma cells. Our study was inspired by increasing numbers of reports that indicate a role for PCs, especially furin and paired basic amino acid cleaving enzyme 4, in tumor progression and metastasis of some solid tumors (Bassi *et al.*, 2005). In this context, it was shown that PC1/3, PC2,

[1]*Laboratory for Neuroendocrinology of the Skin and Interdisciplinary Endocrinology, Department of Dermatology, University of Münster, Münster, Germany;* [2]*Clinical and Experimental Dermatology/Department of Biomedical Sciences, University of Bradford, Yorkshire, UK and* [3]*Institute for Pigmentary Disorders in Association with the E.M. Arndt University of Greifswald, Greifswald, Germany*

Correspondence: Markus Böhm, Laboratory for Neuroendocrinology of the Skin and Interdisciplinary Endocrinology Department of Dermatology, University of Münster, Von-Esmarch-Strasse 58, D-48149 Münster, Germany. E-mail: bohmm@uni-muenster.de

This work is part of the PhD thesis of Nina Weiß.
Spencer JD (2007) H_2O_2-mediated oxidation affects POMC processing and POMC-derived pepides in the human epidermis using vitiligo as a model for oxidative stress. PhD thesis, University of Bradford

Abbreviations: Ab, antibody; AP-1, activator protein-1; ATF6, activating transcription factor 6; CDDE, cell death detection ELISA; dec-RRLL-CMK, decanoyl-RRLL-chloromethylketone; GRP78, glucose-regulated protein 78; MSH, melanocyte-stimulating hormone; NHM, normal human melanocyte; PC, prohormone convertase; SKI-1, subtilisin-kexin isoenzyme-1; siRNA, small interfering RNA; TF, transcription factor; TPA, 12-O-tetradecanoylphorbol-13-acetate

Received 25 June 2012; revised 29 April 2013; accepted 9 May 2013; accepted article preview online 27 June 2013; published online 25 July 2013

and furin are expressed in NHMs (Peters *et al.*, 2000; Spencer *et al.*, 2008). However, little is known about PCs and their potential role in malignant transformation of melanocytes, respectively. Here, we show that SKI-1 is constitutively expressed in pigment cells. Using a small-peptide SKI-1 inhibitor, we were able to pinpoint an essential role of this enzyme in the growth and survival of melanoma cells. On the basis of our observations, we suggest a biological role of SKI-1 in melanoma development. Moreover, our data support SKI-1 as a potential target for melanoma treatment.

RESULTS

Detection of SKI expression and activity in human pigment cells *in vitro*

We first examined the expression of SKI-1 in NHMs and human melanoma cell lines. The latter included WM35 (radial growth phase) and WM902B (vertical growth phase of a primary melanoma); IPC298, A375, G361 (advanced primary melanomas); and SK-Mel-30, IGR37, and WM9 (metastases).

Real-time reverse transcriptase-PCR (RT-PCR) analysis revealed similar mRNA levels of SKI-1 in NHMs and melanoma cells (Figure 1a). The identity of the amplification product in one representative melanoma cell line (IPC298) was confirmed by DNA sequencing and was found to be identical to the mRNA sequence of SKI-1, as deposited in the NCBI (data not shown). Western immunoblotting confirmed these findings. Here, a single band of ~100 kDa was detected. It comigrated with the positive control (HepG2), indicating fully processed SKI-1 (Figure 1b). Notably, SKI-1 protein was also detected in conditioned media of melanoma cells, as shown by one representative melanoma cell line (Figure 1c). Immunofluorescence analysis demonstrated that SKI-1 immunoreactivity is detectable in NHMs as a faint cytoplasmic staining. A speckled immunostaining was also seen in nuclei of NHMs, albeit this staining was more prominent in SK-Mel-30 melanoma cells. By contrast to PC1/3 and PC2 (Peters *et al.*, 2000), SKI-1 did not colocalize in NHMs with the premelanosomal marker NKI/beteb (Figure 1d). In melanoma cells, SKI-1 further colocalized with some melanosomes (Figure 1e). Negative controls consisting of omission of the first antibody (Ab) did not show any staining (data not shown).

To clarify whether the detected SKI-1 in pigment cells is active, we established SKI-1 enzyme assays using the synthetic fluorogenic substrate Ac-RSLK-AMC. Interestingly, SKI-1 activity in conditioned media (Figure 1f), but not in total cell lysates (Supplementary Figure S1 online), was significantly elevated in seven out of the eight melanoma cell lines compared with NHMs.

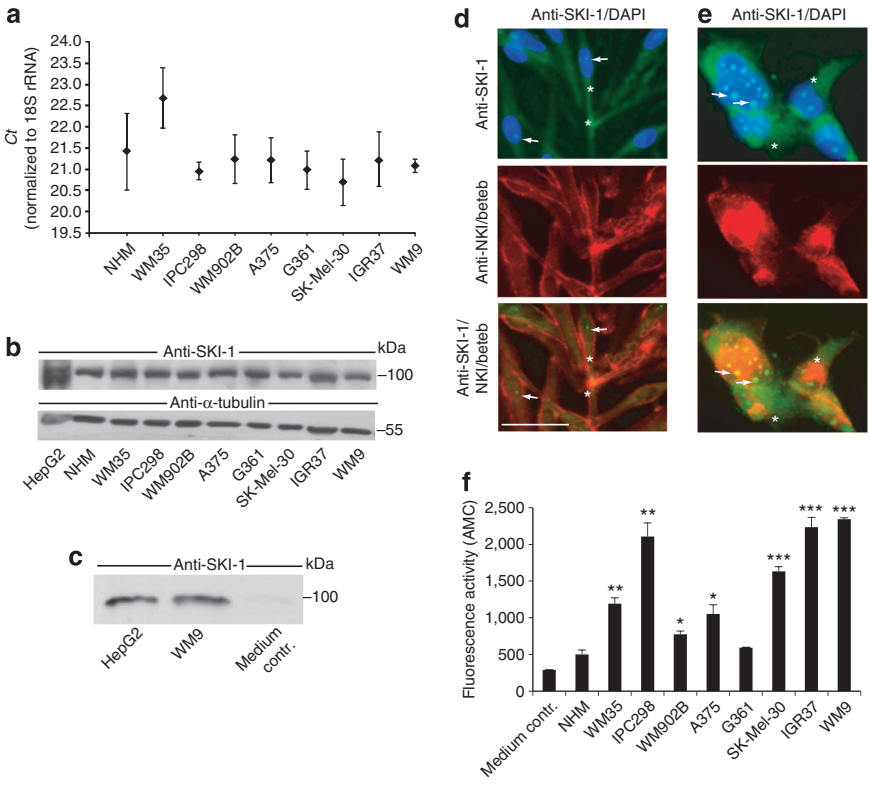

Figure 1. Subtilisin-kexin isoenzyme-1 (SKI-1) expression and activity in human pigment cells *in vitro*. Real-time reverse transcriptase-PCR of SKI-1 in normal human melanocytes (NHMs) and melanoma cell lines; $n = 3$ (**a**). SKI-1 expression in cell lysates of NHMs and melanoma cell lines (15 μg per lane), as shown by western immunoblotting (**b**). Results are based on triplicate experiments. Detection of SKI-1 in conditioned media of melanoma cells as shown by western immunoblotting (40 μg per lane) (**c**). Subcellular localization of SKI-1 in NHMs (**d**) and SK-Mel-30 melanoma cells (**e**), as shown by immunofluorescence analysis. Note cytoplasmic (asterisks) and nuclear SKI-1 immunostaining (arrows). Results are based on triplicate experiments. Bar = 30 μm. SKI-1 activity in conditioned media of NHMs and melanoma cell lines (**f**). Normalized conditioned media were incubated for 3 hours with Ac-RSLK-AMC. $^{*}P<0.05$; $^{**}P<0.01$; $^{***}P<0.001$.

Expression and activity of SKI-1 in normal human skin and metastatic melanoma

Next, we investigated whether SKI-1 expression is altered in human melanoma tissue samples compared with normal skin. Real-time RT-PCR of RNA prepared from cryomaterial of normal skin and melanoma metastases (each $n=5$) disclosed significantly increased mRNA levels of SKI-1 in melanoma tissue (Figure 2a). SKI-1 immunofluorescence analysis of healthy skin ($n=5$) revealed a distinct cytoplasmic staining confined to suprabasal epidermal keratinocytes (Figure 2b). Notably, SKI-1 immunofluorescence was absent in the basal epidermal layer. *In situ* double immunostaining of SKI-1 and NKI/beteb confirmed the absence of SKI-1 in epidermal melanocytes (Figure 2c). However, in accordance with our *ex vivo* SKI-1 mRNA analysis, we detected SKI-1 immunoreactivity in tumor cells of melanoma metastases ($n=5$; Figure 2b and c). Negative controls consisting of replacement of primary Ab with the isotype control confirmed the specificity of this staining (Figure 2b). Moreover, SKI-1 activity was significantly elevated in homogenized tissue samples of melanoma metastases compared with normal skin (each $n=5$; Figure 2d).

Regulation of SKI-1 expression in NHMs

To get a first insight into SKI-1 regulation in pigment cells, we performed *in silico* promoter analysis. We focused on transcription factor (TF)–binding sites that are activated in NHMs by mitogens, proinflammatory signals, and endoplasmic reticulum stress. Consensus sequences in the upstream promoter of SKI-1 were found for cAMP response element binding protein (CREB) (-934; -1309), activator protein (AP)-1 (-2984; -2983; -2723; -2156; -888), NF-κB (-2756; -2383; -2381), and activating transcription factor 6 (ATF6) (-3024; -553) (Supplementary Figure S2a online).

Thus, we determined by RT-PCR the effects of established CREB activators forskolin, α-melanocyte-stimulating hormone (α-MSH), and basic fibroblast growth factor (Böhm *et al.*, 1995; Suzuki *et al.*, 1996; Tada *et al.*, 2002), as well as 12-O-tetradecanoylphorbol-13-acetate (TPA) an activator of protein kinase C and AP-1, on SKI-1 expression in NHMs. Stimulation with forskolin (10 μM), α-MSH (10^{-6} M), and basic fibroblast growth factor (10 ng ml^{-1}) for 3–24 hours did not affect SKI-1 expression (data not shown), whereas TPA decreased SKI-1 levels when stimulated for 6–12 hours (Supplementary Figure S2b online). Exposure of NHMs to

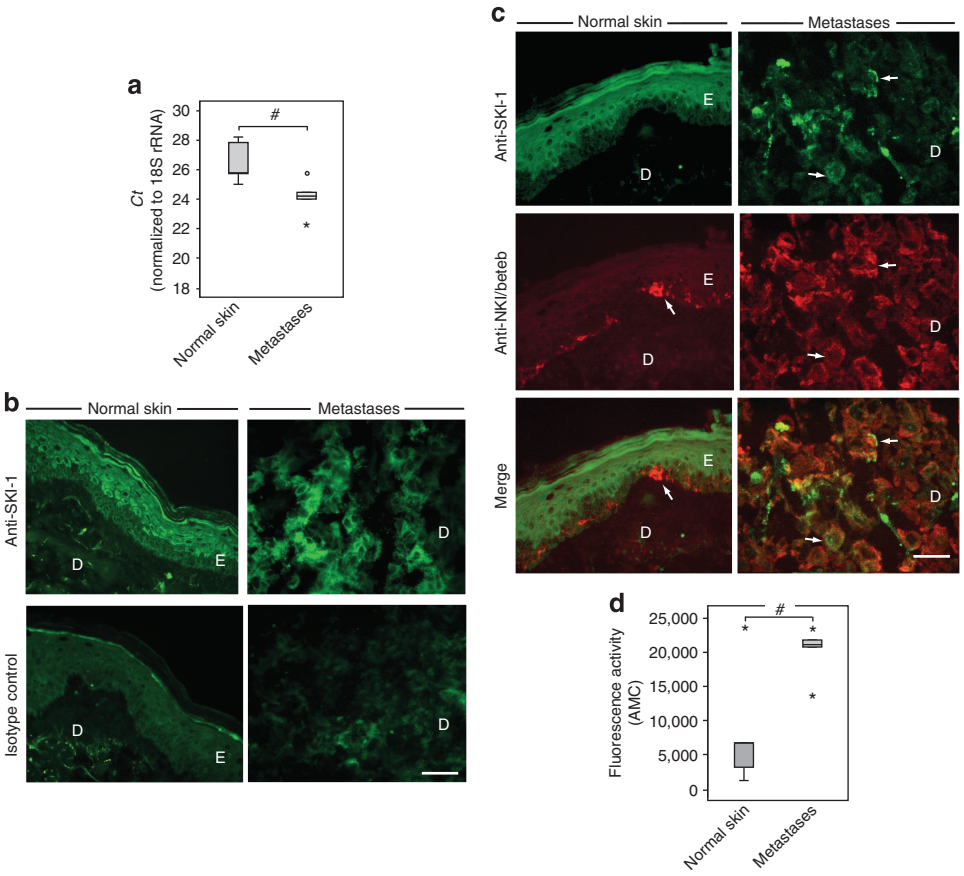

Figure 2. Subtilisin-kexin isoenzyme-1 (SKI-1) expression and activity in normal human skin and melanoma metastases. SKI-1 mRNA levels in tissue samples of normal human skin and melanoma metastases as shown by real-time reverse transcriptase-PCR (**a**), $n=5$ each; $^{\#}P<0.05$. Immunofluorescence analysis of SKI-1 in normal human skin and metastatic melanoma (**b**). One representative set of $n=5$ each is shown. Bar = 30 μm. D, dermis, E, epidermis. Double immunostaining of SKI-1 and NKI/beteb in normal human skin and melanoma metastases (**c**). Bar = 30 μm. Localization of antigens is highlighted by arrows. One representative set $n=5$ each is shown. SKI-1 activity in tissue samples of normal human skin and melanoma metastases (**d**). Tissue lysates ($n=5$ each) were normalized for protein and incubated for 3 hours with the SKI-1 substrate Ac-RSLK-AMC ($^{\#}P<0.05$). NKI, normal human melanocytes.

UVB (10 mJ cm^{-2}, 2–24 hours), IL-1β (1 ng ml^{-1}; 8 hours), or tumor necrosis factor-α (10 ng ml^{-1}, 8 hours), all activators of NF-κB signaling, failed to alter SKI-1 mRNA levels (data not shown). In contrast, the endoplasmic reticulum stressor tunicamycin (Shen and Prywes, 2005) increased SKI-1 mRNA expression after 6–12 hours (Supplementary Figure S2c online).

SKI-1 inhibition suppresses the growth of melanoma cells *in vitro* and *in vivo*

We wondered how SKI-1 inhibition affects human pigment cells, especially melanoma cells. We used the selective and cell-permeable small-peptide inhibitor decanoyl-RRLL-chloromethylketone (dec-RRLL-cmk; Pasquato *et al.*, 2006) to this end. First, we confirmed in one representative melanoma cell line that dec-RRLL-cmk reduces SKI-1 activity *in vitro*. Intracellular SKI-1 activity declined in a dose-dependent manner after treatment of SK-Mel-30 cells with dec-RRLL-cmk for 24 hours (Figure 3a). As early as 30 minutes after dec-RRLL-cmk (50 μM), SKI-1 activity declined and was significantly suppressed after 6 hours to ~10% of control cells (Figure 3b). In accordance with this finding, dec-RRLL-cmk also reduced the expression of glucose-regulated protein 78 (GRP78), which has previously been shown to be regulated by ATF6 via SKI-1 activation (Ye *et al.*, 2000). Accordingly, tunicamycin induced GRP78 expression in SK-Mel-30 cells, and this response was reduced dose dependently by dec-RRLL-cmk (Figure 3c and d).

Next, we examined the *in vitro* effect of dec-RRLL-cmk on proliferation of NHMs and four randomly chosen melanoma cell lines by 2,3-Bis-(2-methoxy-4-nitro-5-sulfophenyl)-2H-tetrazolium-5-carboxanilid-salt and crystal violet assays. Dec-RRLL-cmk had a dose-dependent inhibitory effect on metabolic activity and cell survival of both NHMs and melanoma cells (Supplementary Figure S3a and b online and Figure 4a and b). The IC_{50} values of dec-RRLL-cmk, as measured by crystal violet assay, were 45 μM for NHMs, 33 μM for SK-Mel-30, 25 μM for G361, 29 μM for IPC298, and 34 μM for WM9, suggesting that melanoma cells under the given experimental conditions are more sensitive than NHMs toward the SKI-1

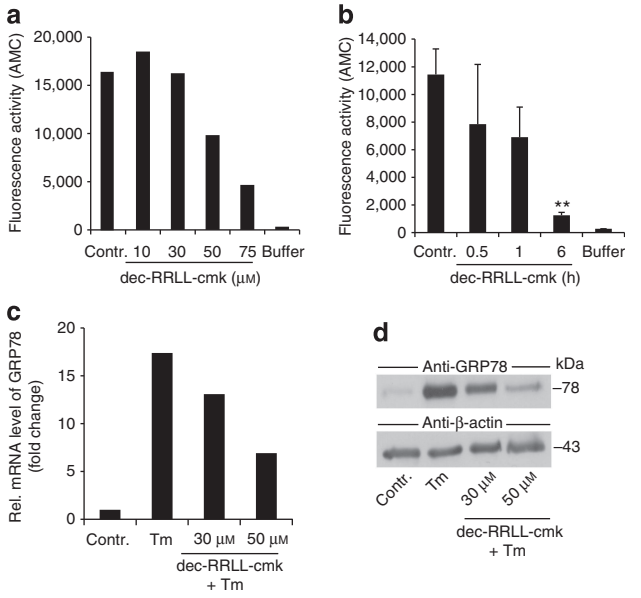

Figure 3. Decanoyl-RRLL-chloromethylketone (Dec-RRLL-cmk) suppresses subtilisin-kexin isoenzyme-1 (SKI-1) activity and reduces glucose-regulated protein 78 (GRP78) expression in melanoma cells. Dose kinetics of dec-RRLL-cmk-mediated suppression of SKI-1 activity in SK-Mel-30 cells (**a**). SKI-1 activity was measured in normalized cell lysates. Depicted is one out of $n=3$ experiments with similar results. Time kinetics of dec-RRLL-cmk-mediated suppression of SKI-1 activity in SK-Mel-30 cells (**b**). Cells were treated with 50 μM dec-RRLL-cmk. Normalized cell lysates were assayed for SKI-1 activity. $n=3$; $^{**}P<0.01$ vs. control. Suppression of GRP78 expression by dec-RRLL-cmk as shown by real-time reverse transcriptase-PCR (RT-PCR; **c**) and western immunoblotting (**d**). Cells were treated with 2 μg ml^{-1} tunicamycin (Tm) for 6 hours (RT-PCR) or 12 hours (western immunoblotting). Dec-RRLL-cmk was preincubated for 1 hour. Panels **c** and **d** are representative sets of three independent experiments. Contr., control.

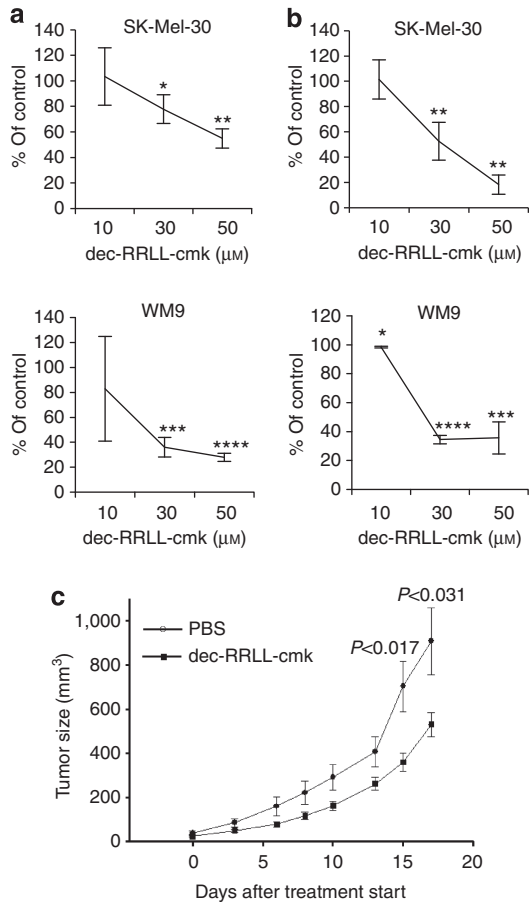

Figure 4. Decanoyl-RRLL-chloromethylketone (Dec-RRLL-cmk) reduces melanoma cell growth *in vitro* and *in vivo*. Metabolic activity was measured by 2,3-Bis-(2-methoxy-4-nitro-5-sulfophenyl)-2H-tetrazolium-5-carboxanilid-salt test where metabolic activity of vehicle-treated cells was set at 100% (**a**). $n=3$; $^{*}P<0.05$, $^{**}P<0.01$, $^{***}P<0.001$, $^{****}P<0.0001$. Cell proliferation was measured by crystal violet assay (**b**). Proliferation of vehicle-treated cells was set at 100%. $n=3$; $^{*}P<0.05$, $^{**}P<0.01$, $^{***}P<0.001$, $^{****}P<0.0001$. Dec-RRLL-cmk reduces melanoma growth in immunodeficient NSG (NOD.Cg-*Prkdc*^{scid} *Il2rg*^{tm1Wjl}/SzJ) mice (**c**). Dec-RRLL-cmk (100 μM) versus phosphate-buffered saline (PBS)/vehicle control was injected three times per week into established tumors (30 mm^3) induced by intracutaneously injected WM9 melanoma cells. $n=7$ mice per treatment group.

inhibitor. To test whether dec-RRLL-cmk can also suppress melanoma cell growth *in vivo*, we injected WM9 melanoma cells intracutaneously into immunodeficient NSG (NOD.Cg-*Prkdc*^{scid} *Il2rg*^{tm1Wjl}/SzJ) mice. Once tumors had a defined size of 30 mm^3, they were injected with the SKI inhibitor (100 μM) or phosphate-buffered saline vehicle as control. In accordance with our *in vitro* data, dec-RRLL-cmk significantly suppressed melanoma growth in this model (Figure 4c).

SKI-1 inhibition induces apoptosis of melanoma cells by a non-ATF6-dependent mechanism

We hypothesized that dec-RRLL-cmk leads to apoptosis of melanoma cells. Giemsa staining of SK-Mel-30 melanoma cells treated with 30 and 50 μM dec-RRLL-cmk for 48 hours indeed disclosed morphological changes reminiscent of apoptosis, e.g., cell shrinkage and nuclear condensation (Figure 5a). Cell death detection ELISA (CDDE) revealed that exposure of melanoma cells to 30–75 μM dec-RRLL-cmk results in a dose-dependent formation of mono- and oligonucleosomes (Figure 5b). This effect was caspase-3-mediated, as processing of poly-adenosine diphosphate-ribose polymerase 1/2 could be detected in cells treated with 50 μM dec-RRLL-cmk for 3 hours (Figure 5b insert). Reprobing of the membrane with an anti-α-tubulin Ab revealed identical amounts of protein in the lanes (data not shown). The apoptosis-inducing effect of dec-RRLL-cmk on melanoma cells was finally confirmed by Annexin-V staining. Dec-RRLL-cmk (50 μM) increased surface expression of phosphatidyl serine comparable to cells treated with staurosporine (Figure 5c).

To clarify the molecular mechanism as to how SKI-1 inhibition by dec-RRLL-cmk leads to apoptosis, we hypothesized that ATF6 is a critical substrate. ATF6 is processed to ATF6α-p50 by SKI-1 (Haze *et al.*, 1999; Pullikotil *et al.*, 2007). Functionally active ATF6α-p50 translocates to the nucleus and binds to ATF6 consensus sequences. Notably, ATF6 was recently reported to exert an essential role in survival of insulinoma cells in the absence of endoplasmic reticulum stress (Teodoro *et al.*, 2012). Therefore, we first examined the impact of dec-RRLL-cmk on ATF6 expression and subcellular localization. In fact, treatment of SK-Mel-30 cells with dec-RRLL-cmk reduced the total protein amounts of processed ATF6, as shown by western immunoblotting using

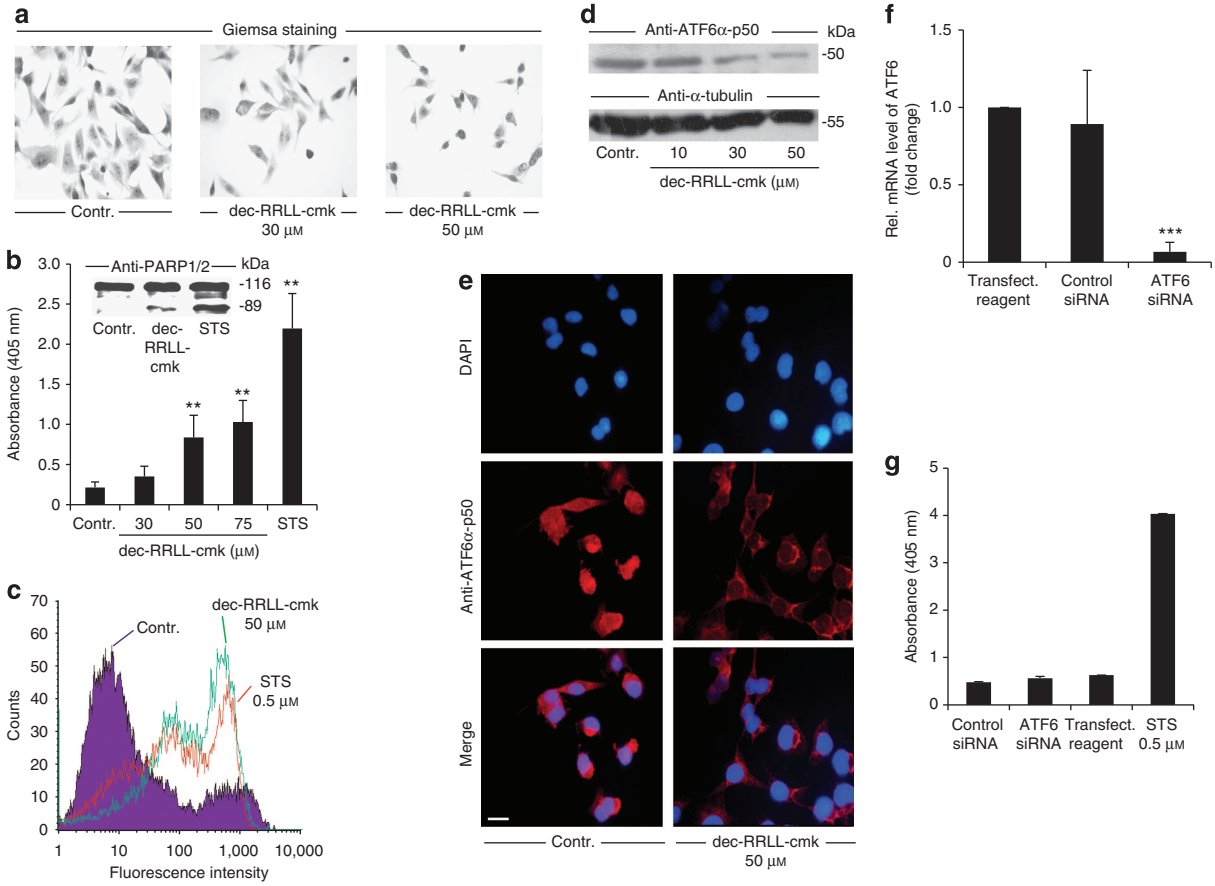

Figure 5. Decanoyl-RRLL-chloromethylketone (Dec-RRLL-cmk) induces apoptosis of melanoma cells independent of ATF6. Morphology of SK-Mel-30 cells after dec-RRLL-cmk treatment (**a**). Dec-RRLL-cmk-mediated apoptosis of SK-Mel-30 cells as shown by cell death detection ELISA (CDDE; **b**) and poly-adenosine diphosphate-ribose polymerase 1/2 (PARP1/2) processing (insert). Cells were treated with dec-RRLL-cmk for 16 hours, followed by CDDE; $n=3$; $^{**}P<0.01$. PARP1/2 processing was determined by western immunoblot after dec-RRLL-cmk (50 μM) or staurosporine (STS) treatment for 3 hours. Dec-RRLL-cmk-mediated apoptosis of SK-Mel-30 cells as shown by Annexin-V staining (**c**). Reduced protein levels and nuclear exclusion of ATF6α-p50 as shown by western immunoblotting (**d**) and immunofluorescence (**e**) in SK-Mel-30 cells after dec-RRLL-cmk. Bar = 10 μm. Small interfering RNA of ATF6 depletes ATF6 levels in WM9 cells, as shown by real-time reverse transcriptase-PCR (**f**), but does not induce apoptosis, as demonstrated by CDDE (**g**). $n=3$; $^{***}P<0.001$. Contr., control.

an ATF6α-p50-specific Ab (Figure 5d). This was paralleled by nuclear exclusion of ATF6α-p50 in cells treated with dec-RRLL-cmk, as highlighted by double immunofluorescent staining (Figure 5e). To test whether depletion of *ATF6* is sufficient to induce apoptosis, we performed gene silencing of *ATF6* using small interfering RNA (siRNA). As transfection of SK-Mel-30 with ATF6 siRNA did not reduce ATF6 mRNA levels (data not shown), we used WM9 cells. Here, 48-hour treatment with a pool of ATF6 siRNA oligonucleotides led to reproducible suppression of ATF6 mRNA expression by >90%. However, *ATF6* gene silencing did not lead to apoptosis in these cells, as shown by CDDE (Figure 5f and g). Other apoptosis read-outs including caspase 3 activity assays also failed to demonstrate induction of apoptosis of WM9 melanoma cells upon *ATF6* gene silencing (data not shown). Similar results were obtained with alternative siRNA ATF6 constructs and with other melanoma cell lines (data not shown). In summary, these findings strongly suggest that apoptosis of melanoma cells induced by dec-RRLL-cmk is independent of ATF6.

DISCUSSION

In this report, we have shown that human pigment cells express SKI-1, a member of the PC family. Although melanocytes are derived from neuroectoderm, our knowledge on PCs in pigment cells is still limited. Previously, PC1/3, PC2, paired basic amino acid cleaving enzyme 4, and furin were detected in NHMs (Peters *et al.*, 2000; Spencer *et al.*, 2008). It was suggested that they process proopiomelanocortin into α-MSH, the latter acting in an autocrine manner in melanocytes and/or in a paracrine manner on epidermal keratinocytes (Slominski, 1991; Moore *et al.*, 1999; Schallreuter *et al.*, 1999). However, the latter PCs are also implicated in the generation of other neurohormones such as β-endorphin or enkephalin (Slominski *et al.*, 2000; Slominski *et al.*, 2011), whereas SKI-1 by means of regulating cholesterol biosynthesis may participate in steroidogenesis within the skin (Slominski *et al.*, 2008).

Our expression analysis of SKI-1 in NHMs and melanoma cells *in vitro* did not reveal differences in SKI-1 expression at first. However, SKI-1 activity was significantly higher in conditioned media of the majority of tested melanoma cell lines than in NHMs. The latter suggest that SKI-1 released by melanoma cells may confer growth advantage presumably by processing and activating a secreted paracrine growth factor or another substance. However, preliminary data with dec-RRLL-cmk-treated WM9 cells indicated that conditioned medium does not abrogate the growth-suppressing effect of the SKI-1 inhibitor *in vitro*.

Notably, in normal human skin SKI-1, expression was localized primarily in suprabasal epidermal keratinocytes, whereas basal keratinocytes and melanocytes were non-reactive. These findings suggest a role of SKI-1 for keratinocyte differentiation. In accordance with our SKI-1 activity assays in melanoma cells *in vitro*, we found SKI-1 mRNA and enzyme activity levels to be significantly elevated in metastatic melanomas compared with normal skin. Further, SKI-1 immunoreactivity was detected in tumor cells of melanoma metastases. Future studies on a larger panel of melanoma specimens are needed to clarify whether SKI-1 expression is related to tumor progression or metastasis.

Our functional studies on SKI-1 in human pigment cells disclosed an essential role for this PC in cell survival. The crucial function of SKI-1 for melanoma cell growth was demonstrated by pharmacological studies using the cell-permeable and highly specific enzyme inhibitor dec-RRLL-cmk in melanoma cells *in vitro*, as well as *in vivo* in immunodeficient mice. It was previously shown that dec-RRLL-cmk at doses of ⩽100 μM specifically inhibits SKI-1 (Pasquato *et al.*, 2006). The prosurvival role of SKI-1 in pigment cells, as highlighted in our study, is supported by others. Cartilage-specific SKI-1 knockout mice displayed an increase in chondrocyte apoptosis in the cartilage (Patra *et al.*, 2007). Future *in vivo* studies will have to further assess the potency of dec-RRLL-cmk on tumor growth and metastasis in melanoma animal models.

With regard to the molecular mechanism of apoptosis mediated by dec-RRLL-cmk, we demonstrated that several SKI-1 substrates/target genes are affected. Co-treatment of SK-Mel-30 cells with the SKI-1 inhibitor plus tunicamycin reduced GRP78 expression compared with tunicamycin alone. Although little is known on the function of ATF6 in melanoma, it was recently shown that siRNA of GRP78 induces apoptosis of melanoma cells (Martin *et al.*, 2010). However, gene silencing of *ATF6* by siRNA failed to induce apoptosis in our hands despite the fact that dec-RRLL-cmk markedly reduced the protein levels of ATF6α-p50. These findings suggest that ATF6—in contrast to insulinoma cells (Teodoro *et al.*, 2012)—does not regulate basal GRP78 expression in melanoma cells. In support of this, basal GRP78 mRNA levels were not altered by treatment of melanoma cells with dec-RRLL-cmk (data not shown). Future studies are thus needed to identify critical target genes or substrates that mediate apoptosis of melanoma cells following SKI-1 inhibition.

MATERIALS AND METHODS

Cells, chemicals, and stimulation

All melanoma cell lines were maintained as described (Li *et al.*, 2004). WM35, WM902B, and WM9 cells were a gift from M. Herlyn (The Wistar Institute, Philadelphia, PA), A375 and G361 were from ATCC (Rockville, ML), and IPC298, IGR37, and SK-Mel-30 cells were from DSMZ (Braunschweig, Germany). NHMs were purchased from Tebu-bio (Portland, OR) and cultured as described (Kokot *et al.*, 2009). Before stimulation with growth factors, NHMs were deprived for 48 hours from TPA or bovine pituitary extract. Dec-RRLL-cmk was from Bachem (Weil am Rhein, Germany), tunicamycin and TPA from Sigma (St Louis, MO), forskolin and α-MSH from Calbiochem (Schwalbach, Germany), basic fibroblast growth factor and tumor necrosis factor-α from Immunotools (Friesoythe, Germany), and IL-1β from Biomol (Hamburg, Germany). UVB irradiation of NHMs was performed as described (Kokot *et al.*, 2009).

RNA extraction, real-time RT-PCR, and sequencing

Standard protocols were used for total RNA preparation from cells and tissue sections, for semiquantitative and real-time RT-PCRs and for DNA sequencing. They are described in the Supplementary

Information online. Expression analysis of SKI-1 in human skin and melanoma samples derived from routine diagnostic and therapeutic procedures was approved by the Local Ethical Committee of the University of Münster. Established primer sets were used for glyceraldehyde-3-phosphate dehydrogenase (Kokot *et al.*, 2009), 18S rRNA (Natarajan *et al.*, 2010), SKI-1 (Dubuc *et al.*, (2004), GRP78 (Yan *et al.*, 2010), and ATF6 (Namba *et al.*, 2007).

ATF6 gene silencing

A pool of four siRNA oligonucleotides (SMARTpool; Thermo Scientific Dharmacon, Bonn, Germany) was used to deplete cells from *ATF6*. Nontargeting control siRNA was used as negative control. Cells were transfected for 48 hours with siRNA at a final concentration of 25 nM according to the manufacturer's instructions.

Western immunoblotting

Routine protocols were used for preparation of cell lysates, SDS-PAGE, western blotting, and immunoprobing (Kokot *et al.*, 2009). For detection of SKI-1 protein in conditioned media, NHMs and melanoma cells were first cultured for 48 hours in TPA-free medium (DermaLife M Basal medium (CellSystems, St Katharinen, Germany)), followed by harvesting of the supernatants, centrifugation, and concentration by Amicon-Ultra Centrifugal Filters 30 K (Millipore, MA). Fractions of ~250 µl were collected and normalized for protein content. The primary Abs were anti-SKI-1 (Santa Cruz Biotechnology, Heidelberg, Germany, H-300, 1 µg ml^{-1}), anti-poly-adenosine diphosphate-ribose polymerase 1/2 (Santa Cruz Biotechnology, H-250, 1:200), anti-GRP78 (Cell Signaling Technology, Danvers, MA, 1:1,000), and anti-ATF6α-p50 (Teodoro *et al.*, 2012; 1:1,000). Equal protein loading was assured by reprobing with an anti-α-tubulin Ab (Oncogene Research Products, San Diego, CA, 1:1,000) or anti-β-actin Ab (Santa Cruz Biotechnology, 1:1,000).

Immunofluorescence analysis *in vitro*

For detection of SKI-1 and ATF6α-p50 by immunofluorescence, 10,000 cells per well were seeded into eight-well chamber slides (Nalge Nunc International, Naperville, IL). Immunostaining procedures are further described in the Supplementary Information. The Abs were anti-NKI/beteb (Caltag Medsystems, Buckinghamshire, UK, 1:30), anti-SKI-1 (kindly provided by Dr NG Seidah, Clinical Research Institute of Montreal, Canada; 1:100), and anti-ATF6α-p50 (Teodoro *et al.*, 2012; 1:100).

Immunofluorescence analysis *in situ*

Cryostat sections were mounted on Superfrost Plus slides (Thermo Scientific, Braunschweig, Germany), air-dried, and fixed in ice-cold acetone for 10 minutes. After washing with 0.1 M TBS-T (DCS Diagnostics, Hamburg, Germany), slides were blocked with 2% BSA diluted in 0.1 M TBS-T for 30 minutes, and incubated for 4 hours with the anti-SKI-1 Ab (Santa Cruz Biotechnology, H-300, 1 µg ml^{-1}) and the anti-NKI/beteb Ab (GeneTex, Irvine, CA, 1:10). After washing, slides were incubated for 1 hour with secondary Abs coupled to FITC (Dako, Hamburg, Germany, 1:50) and Texas red (Dianova, Hamburg, Germany, 1:400), followed by washing and mounting in Vectashield (Vector Laboratories, Burlingame, CA). The sections were viewed with a fluorescence microscope (Carl Zeiss, Oberkochen, Germany). As negative control, rabbit IgG was used at the same concentration as the primary Ab.

In silico promoter analysis

Comparative promoter analysis of SKI-1 was performed with the Java program TOUCAN (Aerts *et al.*, 2005). Further details are provided in the Supplementary Information online.

SKI-1 activity assay

Enzyme assays were performed with Ac-RSLK-AMC (Bachem), which is cleaved by SKI-1 into Ac-RSLK and 7-amino-4-methylcoumarin (AMC). AMC is a fluorescent compound that can be subsequently measured to determine SKI-1 activity. To measure SKI-1 activity, *in vitro* cell lysates were prepared as described (Kokot *et al.*, 2009), whereas conditioned media were processed as described above. To measure SKI-1 activity, *ex vivo* fresh tissue was placed into lysis buffer and homogenized by TissueLyserII (Qiagen, Santa Clarita, CA). All samples were normalized for protein content. Identical protein amounts per sample (cell lysates: 8–25 µg; conditioned media: 20 µg; tissue lysates: 25 µg) were then incubated with prewarmed substrate in the dark for 15 minutes at 37 °C in assay buffer consisting of 25 mM Tris, 25 mM 2-(N-morpholino)ethanesulfonic acid, and 1 mM $CaCl_2$ (pH 7.5). Ac-RSLK-AMC was added to the reaction mixture (total volume 100 µl; final concentration 100 µM). The reaction was stopped at indicated time points with 100 µl of ice-cold 5 mM EDTA. AMC generation was measured with a spectrofluorometer (Infinite M200, Tecan, Männedorf, Switzerland; excitation: 360 nm; emission: 460 nm) against a standard curve generated with AMC (Molekula, Munich, Germany). All samples were assayed in duplicate.

Giemsa staining

Giemsa staining of SK-Mel-30 cells exposed to dec-RRLL-cmk in the presence of 1% fetal calf serum was performed as described before (Ramser *et al.*, 2009).

In vitro growth assays

Metabolic activity and cell proliferation were measured by routine protocols, as outlined in the Supplementary Information online.

Apoptosis assays

Apoptosis was measured by CDDE and Annexin-V FACS analysis as described before (Böhm *et al.*, 2005). All apoptosis read-outs were performed on cells cultured in the presence of 1% fetal calf serum.

In vivo efficacy studies

Animal studies were conducted in immunodeficient NSG (NOD.Cg-*Prkdc*^{scid} *Il2rg*^{tm1Wjl}/SzJ) mice (purchased from Dr Leonard Schultz, The Jackson Laboratory) under institutional approval (animal protocol 8.87–50.10.36.08.286). Mice were used at an age of 8–14 weeks. WM9 melanoma cells (1×10^5 cells per animal) were injected intracutaneously into 14 NSG mice. Tumor size was measured every other day using a caliper. Once tumors had reached a size of 30 mm^3, they were injected three times a week with 20 µl of dec-RRLL-cmk (100 µM; $n = 7$) or phosphate-buffered saline/vehicle ($n = 7$). Mice were killed when tumors had reached a final size of 1 cm^3 or became ulcerated.

Statistical analysis

All experiments were performed at least three times. Statistical significance of the means ± SD or SEM was determined by the Student's *t*-test using Origin 6.0 G (OriginLab, Northampton, MA) or IBM SPSS 20.0 (Dynelytics, Zürich, Switzerland).

CONFLICT OF INTEREST

The authors state no conflict of interest.

ACKNOWLEDGMENTS

This work was supported by a grant from the Innovative Medizinische Forschung to MB and CW. We thank Mara Apel, Meike Steinert, and Andrea Wissel for expert technical assistance.

SUPPLEMENTARY MATERIAL

Supplementary material is linked to the online version of the paper at http://www.nature.com/jid

REFERENCES

Aerts S, Van Loo P, Thijs G *et al.* (2005) TOUCAN 2: the all-inclusive open source workbench for regulatory sequence analysis. *Nucleic Acids Res* 33:393–6

Bassi DE, Fu J, Lopez DC, Klein-Szanto AJ (2005) Proprotein convertases: ''Master switches'' in the regulation of tumor growth and progression. *Mol Carcinog* 44:151–61

Benjannet S, Rhainds D, Essalmani R *et al.* (2004) NARC-1/PCSK9 and its natural mutants: zymogen cleavage and effects on the low density lipoprotein (LDL) receptor and LDL cholesterol. *J Biol Chem* 279: 48865–75

Böhm M, Moellmann G, Cheng E *et al.* (1995) Identification of p90RSK as the probable CREB-Ser133 kinase in human melanocytes. *Cell Growth Differ* 6:291–302

Böhm M, Wolff I, Scholzen TE *et al.* (2005) Alpha-melanocyte-stimulating hormone protects from ultraviolet radiation-induced apoptosis and DNA damage. *J Biol Chem* 280:5795–802

Dubuc G, Chamberland A, Wassef H *et al.* (2004) Statins upregulate PCSK9, the gene encoding the proprotein convertase neural apoptosis-regulated convertase-1 implicated in familial hypercholesterolemia. *Arterioscler Thromb Vasc Biol* 24:1454–9

Espenshade PJ, Cheng D, Goldstein JL *et al.* (1999) Autocatalytic processing of site-1 protease removes propeptide and permits cleavage of sterol regulatory element-binding proteins. *J Biol Chem* 274:22795–804

Gorski JP, Huffman NT, Cui C *et al.* (2009) Potential role of proprotein convertase SKI-1 in the mineralization of primary bone. *Cells Tissues Organs* 189:25–32

Haze K, Yoshida H, Yanagi H *et al.* (1999) Mammalian transcription factor ATF6 is synthesized as a transmembrane protein and activated by proteolysis in response to endoplasmic reticulum stress. *Mol Biol Cell* 10:3787–99

Kokot A, Metze D, Mouchet N *et al.* (2009) α-Melanocyte-stimulating hormone counteracts the suppressive effect of UVB on Nrf2 and Nrf-dependent gene expression in human skin. *Endocrinology* 150:3197–206

Lenz O, ter Meulen J, Klenk HD *et al.* (2001) The Lassa virus glycoprotein precursor GP-C is proteolytically processed by subtilase SKI-1/S1P. *Proc Natl Acad Sci USA* 98:12701–5

Li Z, Metze D, Nashan D *et al.* (2004) Expression of SOCS-1, suppressor of cytokine signalling-1, in human melanoma. *J Invest Dermatol* 123:737–45

Martin S, Hill DS, Paton JC *et al.* (2010) Targeting GRP78 to enhance melanoma cell death. *Pigment Cell Melanoma Res* 23:675–82

Moore J, Wood JM, Schallreuter KU (1999) Evidence for specific complex formation between alpha-melanocyte stimulating hormone and 6(R)-L-erythro-5,6,7,8-tetrahydrobiopterin using near infrared Fourier transform Raman spectroscopy. *Biochemistry* 138:15317–24

Namba T, Ishihara T, Tanaka K *et al.* (2007) Transcriptional activation of ATF6 by endo-plasmic reticulum stressors. *Biochem Biophys Res Commun* 355:543–8

Natarajan VT, Singh A, Kumar AA *et al.* (2010) Transcriptional upregulation of Nrf2-depemdent phase II detoxification genes in the involved epidermis of vitiligo vulgaris. *J Invest Dermatol* 130:2781–9

Pasquato A, Pullikotil P, Asselin MC *et al.* (2006) The proprotein convertases SKI-1/S1P. *In vitro* analysis of the lassa virus glycoprotein-derived substrates and *ex vivo* validation of irreversible peptide inhibitors. *J Biol Chem* 281:23471–81

Patra D, Xing X, Davies S *et al.* (2007) Site-1 protease is essential for endochondral bone formation in mice. *J Cell Biol* 179:687–700

Peters EM, Tobin DJ, Seidah NG *et al.* (2000) Pro-opiomelanocortin-related peptide, prohormone convertase 1 and 2 and the regulatory peptide 7B2 are present in melanosomes of human melanocytes. *J Invest Dermatol* 114:430–7

Pullikotil P, Benjannet S, Mayne J *et al.* (2007) The proprotein convertase SKI-1/S1P: alternate translation and subcellular localization. *J Biol Chem* 282:27402–13

Ramser B, Kokot A, Metze D *et al.* (2009) Hydroxychloroquine modulates metabolic activity, proliferation and induces autophagic cell death of human dermal fibroblasts. *J Invest Dermatol* 129:2419–26

Schallreuter KU, Moore J, Tobin DJ *et al.* (1999) Alpha-MSH can control the essential cofactor 6-tetrahydrobiopterin in melanogenesis. *Ann NY Acad Sci* 885:329–41

Schlombs K, Wagner T, Scheel J *et al.* (2003) Site-1 protease is required for cartilage development in zebrafish. *Proc Natl Acad Sci USA* 100:14024–9

Seidah NG, Chrétien M (1999a) Proprotein and prohormone convertases: a family of subtilases generating diverse bioactive polypeptides. *Brain Res* 848:45–62

Seidah NG, Mowla SJ, Hamelin J *et al.* (1999b) Mammalian subtilisin/kexin isozyme SKI-1: a widely expressed proprotein convertase with a unique cleavage specificity and cellular localization. *Proc Natl Acad Sci USA* 96:1321–6

Seidah NG, Prat A (2007) The proprotein convertases are potential targets in the treatment of dyslipidemia. *J Mol Med* 85:685–96

Seidah NG (2011) The proprotein convertases, 20 years later. *Methods Mol Biol* 768:23–57

Shen J, Prywes R (2005) ER stress signaling by regulated proteolysis of ATF6. *Methods* 35:382–9

Slominski A (1991) POMC gene expression in mouse and hamster melanoma cells. *EBS Lett* 291:165–8

Slominski A, Wortsman J, Luger TA *et al.* (2000) Corticotropin releasing hormone and proopiomelanocortin involvement in the cutaneous response to stress. *Physiol Rev* 80:979–1020

Slominski A, Wortsman J, Paus R *et al.* (2008) Skin as an endocrine organ: implications for its function. *Drug Discovery Today: Dis Mech* 5:e137–44

Slominski AT, Zmijewski MA, Zbytek B *et al.* (2011) Regulated proenkephalin expression in human skin and cultured skin cells. *Invest Dermatol* 131:613–22

Spencer JD, Gibbons NC, Böhm M *et al.* (2008) The Ca^{2+}-binding capacity of epidermal furin is disrupted by H_2O_2-mediated oxidation in vitiligo. *Endocrinology* 149:1638–45

Suzuki I, Cone R, Im S *et al.* (1996) Binding capacity and activation of the MC1 receptors by melanotropic hormones correlate directly with their mitogenic and melanogenic effects on human melanocytes. *Endocrinology* 137:1627–33

Tada A, Pereira E, Beitner-Johnson D *et al.* (2002) Mitogen- and ultraviolet-B-induced signaling pathways in normal human melanocytes. *J Invest Dermatol* 118:316–22

Teodoro T, Odisho T, Sidorova E *et al.* (2012) Pancreatic β-cells depend on basal expression of activeATF6α-p50 for cel survival even under nonstress conditions. *Am J Physiol Cell Physiol* 302:992–1003

Yan Y, Gao YY, Liu BQ *et al.* (2010) Resveratrol-induced cytotoxicity in human Burkitt's lymphoma cells is coupled to the unfolded protein response. *BMC Cancer* 10:445

Yang J, Goldstein JL, Hammer RE *et al.* (2001) Decreased lipid synthesis in livers of mice with disrupted Site-1 protease gene. *Proc Natl Acad Sci USA* 98:13607–12

Ye J, Rawson RB, Komuro R *et al.* (2000) ER stress induces cleavage of membrane-bound ATF6 by the same proteases that process SREBPs. *Mol Cell* 6:1355–64